

## SEISMIC RISK EVALUATION BASED ON MAXIMUM LIKELIHOOD TECHNIQUE APPLIED FOR THE RED SEA REGION

By

ADEL A. A. OTHMAN

Department of Geology, Faculty of Science, University of Qatar, Doha, Qatar  
Permanent Address: Al-Azhar University, Faculty of Science, Geology Department, Nacr City, Cairo, Egypt

### تقييم الخطر الزلزالي باستخدام تقنية التشابه العظمي لمنطقة البحر الأحمر

عادل علي عثمان

أجري تحليل للخطر الزلزالي لمنطقة البحر الأحمر للزلازل المسجلة في المنطقة في الفترة ما بين الأول من يناير ١٩١٣م حتى نهاية ٣١ ديسمبر ١٩٨٢م ، وقد استخدمت طريقة التشابه العظمي لتحديد معاملات الخطر في المنطقة . وقد حسبت قيم الخطر ورسمت لأزمنة تصميم مختلفة مثل ١ ، ١٠ ، ٢٠ ، ٣٠ ، ٤٠ ، ٥٠ ، ١٠٠ عام على التوالي .

وقد نتج عن الدراسة أن قيم الخطر المتوقعة عالية لأزمنة التصميم الطويلة مثل ١٠٠ عام أو أكثر والتي تنجم من زلازل لها الضخامة ٦ أو أعلى . ولقد تراوحت قيم الخطر الزلزالي المتوقعة من ١٥٪ لزمّن تصميم يساوي عام واحد إلى ١٠٠٪ لزمّن تصميم ١٠٠ عام .

*Key Words:* Seismic risk, return time, earthquake magnitude.

#### ABSTRACT

An analysis of the seismic risk is carried out for the Red Sea region for the recorded earthquakes in the area between 1. January 1913 and 31 December 1982. The maximum likelihood method was applied to determine the hazard parameters of the area. The risk valued are calculated and plotted for different design time as 1, 10, 20, 30, 40, 50, and 100 years, respectively.

The estimated risk values are high for higher design times like 100 years or more, which is produced from earthquakes of magnitudes equal or higher than 6.0. The estimated risk values ranged from 15% for  $R_D=1$  year up to 100% for  $R_D=100$  years.

#### INTRODUCTION

The Red Sea is of particular interest to geosciences because it is thought to be a region where sea floor spreading is presented in its early stages, as well as the sea itself having formed by a separation of the African and Arabian continental block. This spreading caused plate movements which is one of the important reasons for earthquakes generation.

The need to evaluation the seismic risk of a region is increased when an important structure or disaster emergency planning is applied. At present, intensive urban and industrial development is being undertaken in the Red Sea region and therefore the estimation of seismic risk parameters is needed. In the present work, historical and observational data on seismic events in the Red Sea region have been studied and analyzed for evaluation of seismic risk. The maximum likelihood technique is applied to estimate the earthquake

hazard parameters like maximum regional magnitude ( $m_{max}$ ), activity rate ( $\lambda$ ) and  $\beta$  (the magnitude-frequency distribution parameter).

Many authors discussed the seismic risk in different localities. Mertz and Cornell (1973) developed an analytical relationship applying quadratic log frequency versus magnitude to analyze the engineering seismic risk. They computed the seismic risk for a fault-site configuration. Caputo (1974) calculated the seismic risk in Italy region. Lomnitz (1974) applied the extreme-value technique to study the seismic risk for the state of California, USA. Burton (1978) studied the seismic hazard of England based on recurrence statistics of the extreme values of earthquakes. Barazangi (1981) reported the earthquake activity in the western part of the Arabian Plate for 200-300 Km towards the interior of the plate from the tectonically active Red Sea rift system. He suggested the existence of an appreciable seismic

risk in the western region of Arabian without any estimations. Hattori and Ibrahim (1981) evaluated the seismic risk in and around Egypt for the period B.C. 2200 - A.D. 1978. They applied the method of extreme values. For seismic risk mapping they applied a return period of 300 and 600 years. Kijko and Dessokey (1987) applied the extreme magnitude distribution to incomplete earthquake files. Kijko and Sellevoll (1990), applied a new technique using the maximum likelihood method. Prochazkova *et al.* (1990) studied the earthquake hazard of northern parts of the Bohemian Massif.

RISK STATISTICS

For a general statistical analysis of earthquake activity it is necessary to assume that the earthquakes are independent events. It is also assumed that the pattern of earthquake occurrence is time invariant. This will be true for historical time spans but not necessarily true for geological time spans (Burton, 1978).

The statistical procedure developed by Kijko and Sellevoll (1990) is used to distinguish the parts of the catalog containing only the information on the extremal earthquakes and the complete information on earthquakes whose magnitudes or epicentral intensities are greater or equal to a certain level. This procedure of earthquake risk evaluation does not require that the extreme earthquake epicentral intensity or the magnitude distribution in equal time intervals be known (Prochazkova *et al.*, 1990).

LIKELIHOOD TECHNIQUE FOR SEISMIC RISK EVALUATION

The assumption of the Poisson's occurrence of earthquakes with activity rate  $\lambda$  and of the doubly truncated Gutenberg-Richter distribution  $F(x)$  of earthquakes of magnitude  $x$  is an important basis of the technique.

The doubly truncated exponential distribution can be represented as:

$$F(x) = P_r(X \leq x) = [A_1 - A(x)] / [A_1 - A_2], m \leq x \leq m_{max} \quad (1)$$

where:

$$A_1 = \exp(-\beta m_{min})$$

$$A_2 = \exp(-\beta m_{max})$$

$$A(x) = \exp(-\beta x)$$

$m_{max}$  is the maximum regional magnitude value.  $m_{min}$  is the threshold magnitude, and  $\beta$  is a parameter characterizing magnitude frequency distribution. The above assumption implies that earthquakes of magnitudes greater than  $x$  can be represented by a Position process with the mean rate of occurrence  $\lambda(1-F(x))$ , where  $\lambda$  is the activity rate corresponding to the threshold magnitude  $m_{min}$ . Thus, the probability that  $X$ , the largest magnitude within a period of  $t$  years, will be less than some specified magnitude  $x$  is given by:

$$G(x|t) = P_r(X \leq x)$$

$$= \exp(-\lambda t [(A_2 - A(x))(1-F(m_0)) / A_2 - A_3]) \quad (2)$$

where:

$$A_3 = \exp(-\beta m_0)$$

$m_0$  is the threshold magnitude for the extreme part of the catalog and  $m_0 \geq m_{min}$ . The last probability is a doubly truncated expression. From  $A_3$  and  $A_2$  and according to the following conditions:

$m_{max} \rightarrow \infty, A_2 \rightarrow 0$ , and for  $m_0 = m_{min} = 0; A_3 = 1$ . Thus, for  $A_3 = 1$ , and  $A_2 = 0$ , and  $t = 1$ ; equation (2) becomes:

$$G(X) = \exp(-\lambda \exp(-\beta x)) \quad (3)$$

which is equivalent to the first Gumbel's asymptote extremes.

The data for determination of seismicity parameters are the largest earthquake magnitudes  $x_0 = (x_{01}, x_{02}, \dots, x_{0n})$  selected from the first part of the catalog, from the time intervals  $t = (t_1, t_2, \dots, t_{n0})$ . The seismicity parameters sought are  $\xi = f(\beta, \lambda)$  and  $m_{max}$ . From equation (2) it follows that the likelihood function  $\xi$  for extreme magnitude is:

$$L_0(\xi | x_0) = \prod_{i=1}^{n_0} g(\lambda_{0i}, t_i | \xi) \quad (4)$$

where:

$$\ln g(x, t | \xi) = [(A_2 - A(x)) / (A_1 - A_2)] + \ln [\beta \lambda t (1 - F(m_0)) / (A_1 - A_2)] - \beta x \quad (5)$$

ESTIMATION OF SEISMIC RISK PARAMETERS

Applying the maximum likelihood technique, the seismic risk parameters  $\beta$  and  $\lambda$  will be estimated. The likelihood function (L) for extreme and complete parts of the given data can be expressed as follows:

$$L(\xi | x) = \prod_{i=0}^s L_i(\xi | x_i) \quad (6)$$

Following the maximum likelihood solution of Kijko and Sellevoll (1990), for magnitudes between  $x^L$  and  $x^H$ , which L means low and H means high, a set of equation may be obtained as:

$$A_4^{EXT} + A_4^{COMP} = 0 \quad (7)$$

$$A_5^{EXT} + A_5^{COMP} = 0 \quad (8)$$

where:

$$A_4^{EXT} = - \sum_{j=1}^{n_0} t_j \frac{G(x_{0j}^L | t_j) H(x_{0j}^H) - G(x_{0j}^H | t_j) H(x_{0j}^L)}{G(x_{0j}^L | t_j) - G(x_{0j}^H | t_j)}$$

$$A_5^{EXT} = \lambda \sum_{j=1}^{n_0} t_j \frac{G(x_{0j}^L | t_j) B(x_{0j}^H) - G(x_{0j}^H | t_j) B(x_{0j}^L)}{G(x_{0j}^L | t_j) - G(x_{0j}^H | t_j)}$$

$$A_4^{COMP} = \frac{n_c}{\lambda} - \sum_{i=1}^s T_i H(m_i)$$

$$A_5^{COMP} = \sum_{i=1}^s (D_{1i} + D_{2i})$$

with,

T is the span period and,

$$B(x) = C(m_{\min}, m_{\max})F(x) - E(m_{\min}, x)$$

$$C(x, y) = [xA(x) - yA(y)] / [A(x) - A(y)]$$

$$D_{ji} = n_i C(m_i, m_{\max}) - \sum_{j=1}^n C(x_{ij}^I, x_{ij}^{II})$$

$$D_{2i} = \left[ \lambda T_i - \frac{n_i}{H(m_i)} \right] B(m_i)$$

$$E(x, y) = \frac{xA(x) - yA(y)}{A(x) - A(y)}$$

$$H(x) = 1 - F(x)$$

is a complemented cumulative probability function.

$$n_c = \sum_{i=1}^s n_i$$

is the number of

earthquakes in the complete part of the catalog. The indexes COMP and EXT are for the complete part and the extreme of the catalog, respectively.

For a given  $m_{\max}$ , equations (7) and (8) can be solved for  $\lambda$  and  $\beta$  by an iteration technique. The maximum likelihood technique does not evaluate  $m_{\max}$ . Therefore, the  $m_{\max}$  estimation must be performed by applying the following conditions, as stated by Kijko and Sellevoll 1990:

$$x_{\max} = \text{Expect}(x_{\max} | T) \quad (9)$$

which means that the largest observed magnitude  $x_{\max}$  is equal to  $\text{Expect}(x_{\max} | T)$ , the largest expected magnitude in the span of the catalog T. According to Kijko (1988), the largest expected magnitude in the time interval T is:

$$\text{Expect}(x_{\max} | T) = m_{\max} - \frac{E_1(TZ_2) - E_1(TZ_1)}{\beta \exp(-TZ_2)} - m_{\min} \exp(-\lambda T) \quad (10)$$

where:  $Z_i = -\lambda A_i / (A_2 - A_1)$   $i = 1, 2$ .  $E_1(TZ_1)$  and  $E_1(TZ_2)$  are exponential integral function, while the span of the catalog consists of two parts, the extreme  $T_0 = \sum_{i=1}^n T_i$  and the complete  $\sum_{i=1}^s T_i$ . Equations (7) to (10) provide three equations for the estimation of  $\beta$ ,  $\lambda$  and  $m_{\max}$ .

### RED SEA REGION

The red Sea is about 1940 km in length and between 280 and 320 km wide stretching out in a NW-SE direction. At its southeastern part the Red Sea joins the Indian Ocean through the Gulf of Aden, and at its northwestern end the Red Sea bifurcates into the Gulf of Suez, extending in the same direction. The Gulf of Aqaba strikes off in a NE direction. The Red Sea may be viewed as a great elongated depression, separating the massifs of the Arabian subcontinent from those forming the backbone of the Eastern Desert of Egypt, the Sudan, Eritrea, and Ethiopia, while the center of this depression is filled with sea water. The country on either side

is chiefly made up of rocks of Miocene and younger age (Said, 1969). It is only along both sides of the Gulf of Suez, the northern end of the red Sea and a small area along the coast of Jiddah that the relief is broken by elongated ridges composed of Cretaceous or Eocene strata with occasional outcrops of basement rocks or older sediments (Said, 1969).

In the Red Sea area, there is a structural relationship between the high lands of the Arabian-Nubian shield, the sediment-filled Red Sea graben system and the marginal sedimentary cover with large areas of volcanic activity. Among five major systems of faults affecting the Arabian-Nubian massif, three systems trending N, NW, and WNW appear to have a profound influence on the structure of the Red Sea. The other systems are oriented in the NE and E directions. The fissure systems control the coastal lines, and major physiographic features such as depressions, drainage lines, and much of the Nile valley (Abdel-Gawad, 1969).

The Red Sea region is one of the areas around the world which is well investigated geophysically. It has positive Bouguer anomalies indicating the presence of intrusive rocks beneath the deep water. Over the center, there are a large magnetic anomalies; these are probably associated with material with seismic velocities of 4.1 ~ 0.4 km/s overlying material with velocity 7.1 km/s (Heirtzler and Le Pichon, 1965). Near the margins, seismic velocities of about 6 km/s are found suggesting the presence of downfaulted basement (Girdler, 1969).

Seismicity and the interpretation of magnetic anomalies all suggest that the newest crust is under the center of the Red Sea. The magnetic anomalies suggest that over the last few million years the center of the Red Sea has been opening symmetrically at about 1cm/yr. It seems likely that Arabia was moving away from Africa and there was a sequence of crustal thinning, rifting, and crustal separation accompanied by basic intrusions in the formation of the Red Sea

### DESCRIPTION OF DATA AND METHOD

Seismic hazard assessment requires knowledge of the spatial and temporal distribution of earthquake sources. Riad and Meyers (1985) produced a map which shows the spatial distribution of reported shocks in the middle east region. They reported the earthquakes in a manual per geographic areas. The present study depends mainly upon the collected data as they appeared in that manual. Much of the data extracted from these sources still remains microseismic in nature. For each reported earthquake it is possible to assign a maximum intensity. If both depth and area are known, then an estimate of earthquake size or magnitude may be made.

Figure (1), shows the distribution of earthquakes which have an  $m_b$  magnitude to be greater than 3.1. These larger events are the major source to the observed distribution of maximum magnitude and about one such event is expected each year.

### RED SEA EARTHQUAKES

The available registered quakes in the Red Sea region are shown in Fig. (1). It is clear to observe that the middle part of

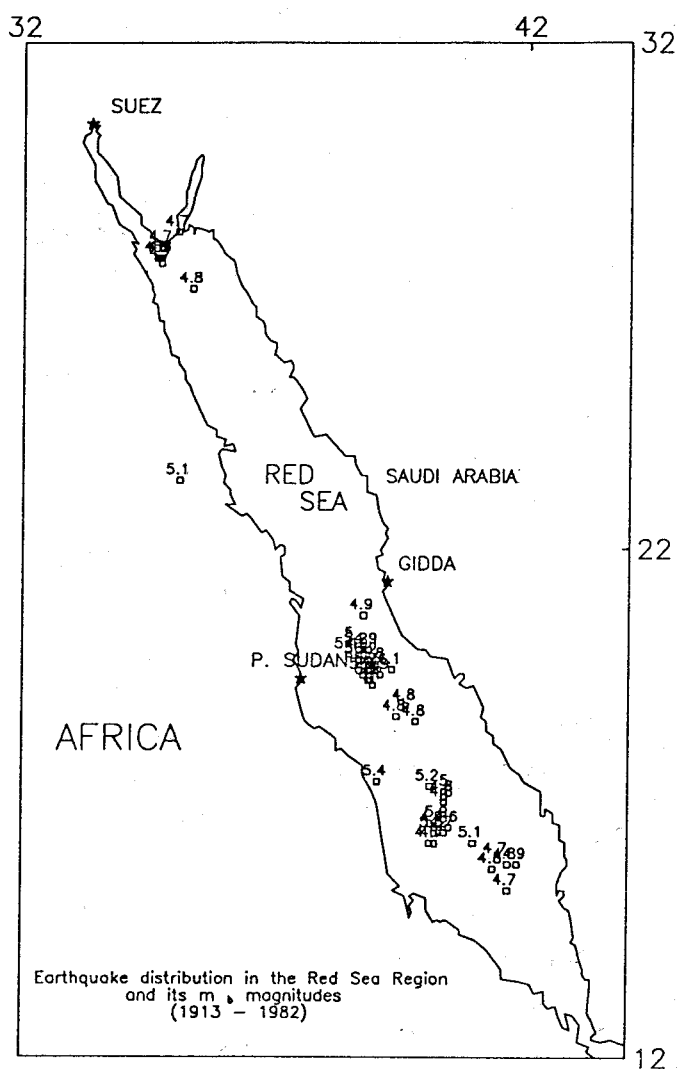


Fig. 1: Distribution of the catalogued earthquakes in the Red Sea area and their magnitude in the period from 1913 to 1982.

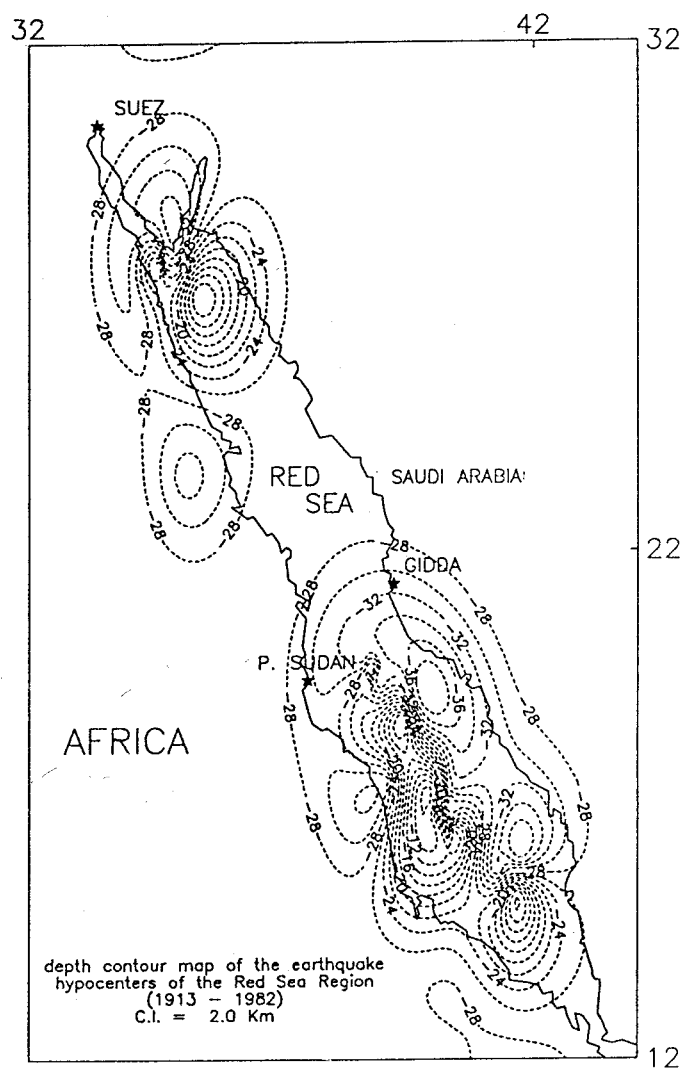


Fig. 2: Depth contour map for the earthquake hypocenters in the Red Sea area.

the Red Sea region between Portsudan, on the western bank of the sea, and Gidda on the eastern coast of it, is rich in earthquakes and has a high concentrated number of the available earthquakes in the studied area. The depth of the epicenters of the quakes are also mapped and plotted in Fig. (2), which ranges 15 kms to about 32 kms under the sea level. This is clearly seen from a representative profile through the Red Sea. Figure (3) shows the depth of these earthquakes along this profile trending from its SE-end of coordinates 34.88 E and 27.70 N to the NE-end of coordinates 42.75 E and 13.45 N, along the Red Sea. According to the lack of the recorded earthquakes, the resolution of these earthquake representation in the profile is of low nature. The earthquakes may be divided into two major groups in terms of depth characteristics. Shallow earthquakes of depth equal to about 10 kms, as shown in Fig. (3), and the deep quakes located at depths of about 33 kms.

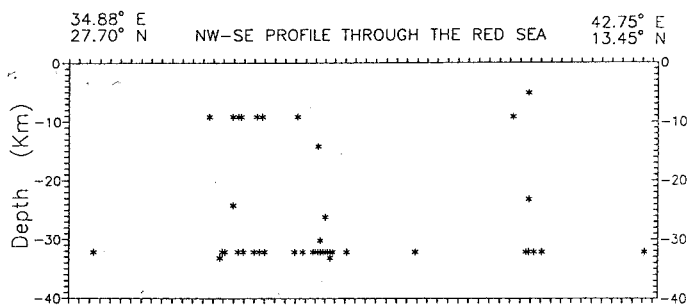


Fig. 3: A generalized profile running from the south part to the north part of the Red Sea. The earthquakes show two major groups at depths equal 8.0 and 32.0 kilometers.

#### RISK PARAMETERS FOR THE RED SEA AREA

The estimation of seismicity parameters and seismic hazard applying the above described technique is executed for

the Red Sea region limited by the latitudes 12° to 32° north and longitudes 32° to 44° east. Random magnitudes were generated according to the doubly truncated Gutenberg-Richter distribution (eq. 1), for parameters  $\beta=2.0$ ,  $m_{min}=3.10$  and  $m_{max}=6.2$  considering the catalog as one complete part. In each operation the same number of earthquakes has been simulated and perturbed by random noise. We used the time interval equal to one year.

The catalog contains 62 earthquakes felt along the red Sea area(see Fig. 1) for the period from 1 January 1913 to 31 December 1982. The estimated parameters for the area using the maximum likelihood technique are:

$$\beta = 1.71 \pm 0.25$$

$$\lambda = 11.12 \pm 4.13 \quad (\text{for } m_{min} = 3.1)$$

$$m_{max} = 6.70 \pm 0.36 \quad (\text{for } \sigma_{x_{max}} = 0.25)$$

The relation between the return time and the earthquake magnitudes are shown in Fig. (4). The mean return time means that a certain magnitude will not be exceeded in any year for the studied area. The  $m_{max}$  may be estimated from the asymptotic line of the magnitude return time curve and equals 6.7, as shown in Fig. (4).

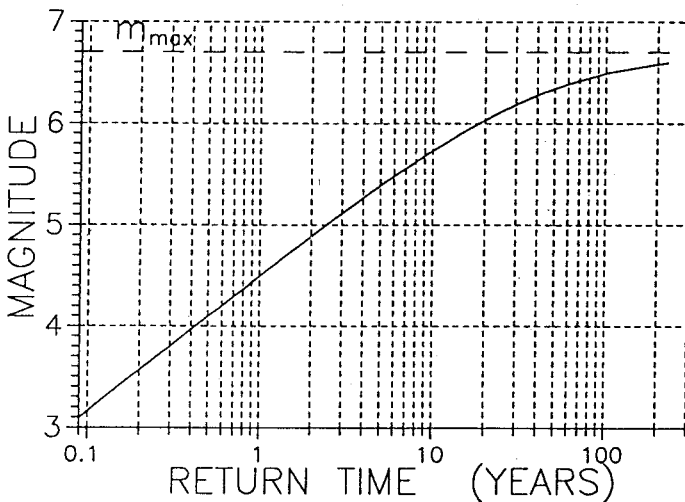


Fig. 4: Return time in years of the studied earthquakes as function of its magnitudes calculated by maximum likelihood method, which shown an maximum magnitude at 6.7.

### SEISMIC RISK EVALUATION

Applying the results of the above mentioned algorithm to calculate the return times of the earthquake magnitude in the region, the seismic risk would be estimated. The seismic risk  $R(x)$  for an earthquake of a magnitude  $x$  is evaluated according to the following equation (Lomnitz, 1974) as:

$$R(x) = 1 - e^{-\frac{T_D}{T_R(x)}} \quad (11)$$

SEISMIC RISK FOR DESIGNED TIMES:  
1 , 10 , 30 , 50 , 100 YEARS

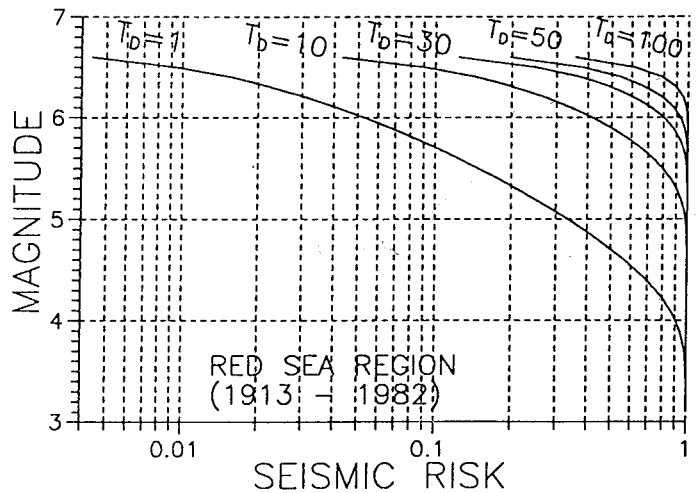


Fig. 5: Computed seismic risk for the Red Sea region at different designe times. These designe times are 1, 10, 30, 50, and 100 years for the time period 1913-1982.

where  $T_D$  is the designed time of a structure and  $T_R(x)$  is the return time of an earthquake of magnitude  $x$ . Figure (5) describes the relation between the magnitudes and the estimated seismic risk for the Red Sea region at different designe times equal to 1, 10, 40, 50, and 100 years, respectively. As shown in the figure, the seismic risk increased as the magnitude of the earthquake decreased. It is also clear that the seismic risk increases by increasing the designe times. Rate of increasing the risk values is increased by increasing the designe time. This means that if you construct a structure designed for a time longer than 100 years, its risk will be higher than one of smaller designe times. The relation for  $T_D = 1$  year, as displayed in Fig. (5), declares that the higher probable risk is for the earthquakes of lower magnitudes which means that its repetition is more probable than that for higher magnitudes. The case is different for  $T_D=100$  years, which shows dramatic increase of the evaluated risk especially for high magnitudes. It is clear that higher magnitudes cause higher seismic risk values and vise versa, i.e. the small magnitudes cause a small risk for the near structures.

The spatial distribution of the evaluated seismic risk in the studied area is shown in the figures 6 to 11. In Fig. (6), a contour map displays the risk for designe time equal to one year. The minimum value of the estimated risk is 0.15 and found south of Gidda, and the maximum value which equals 0.50 is found to be in the south part of the Red Sea and also at the opening of the Gulf of Suez, near Shidwan Island area, at the north of the Red Sea. The estimated risk for the designe time 10.0 years is some different than the last distribution which concentrates the lower values between south of Gidda and east of Port Sudan cities. Its values range starting from 0.50 up to more than 0.90 at both northern- and southern-parts of the Red Sea as shown in Fig. (7). For the time 20.0 years, Fig. (8) shows the contours of risk values which start at about 70% south of Gidda and reach 85% near Gidda and about 95% east of Port Sudan. The observed difference in risk values is not large in case of a designe time equal to 30.0 years as

displayed in Fig. (9). The smallest risk value equals to 80% and increased up to 95% towards Gidda and Port Sudan, as shown in Fig. (9). The next figures (10 and 11) show a higher risk starting at 90% for design times 40 and at 91% for 50 years. In general, it is clear that the region between Gidda and Port Sudan features higher risk values and these values increase by increasing the design times for a structure or an industrial large project.

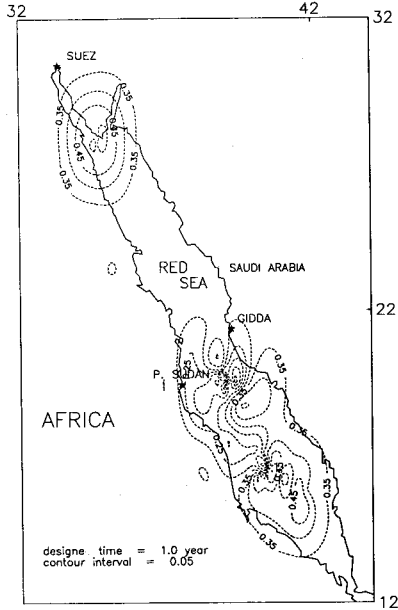


Fig. 6: Seismic risk contour map for the design time equal to one year. The contours show a low risk values all over the region.

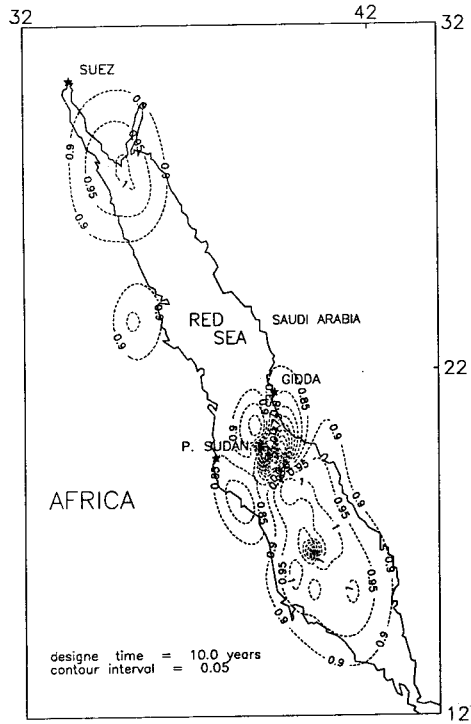


Fig. 8: Calculated risk values for design time equal to 20.0 years. The more probable areas of high risk are centered south of Gidda and eastward of Ports Sudan, in the middle part of the Red Sea.

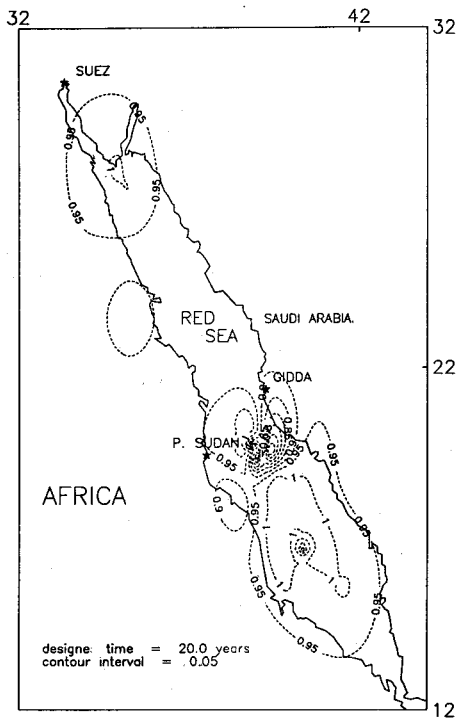


Fig. 7: Seismic risk values of the design time 10 years. The middle part of the Red Sea displays a high risk value but the northern and southern parts are even of higher one.

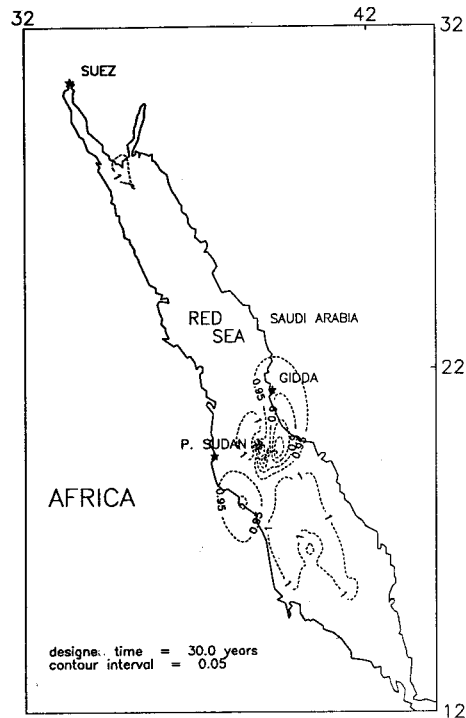


Fig. 9: Seismic risk map for the design time of 30.0 years with high values concentrated south of Gidda and east of Port Sudan.

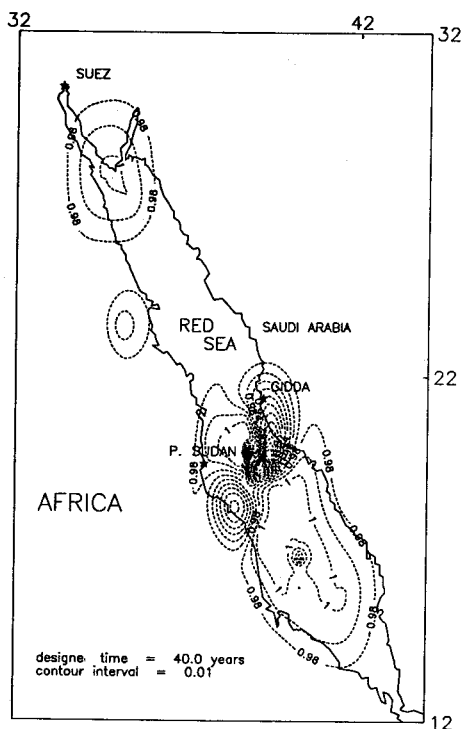


Fig. 10: Higher risk values are shown near Gidda in the middle part of the Red Sea, calculated at design time equal to 40.0 years.

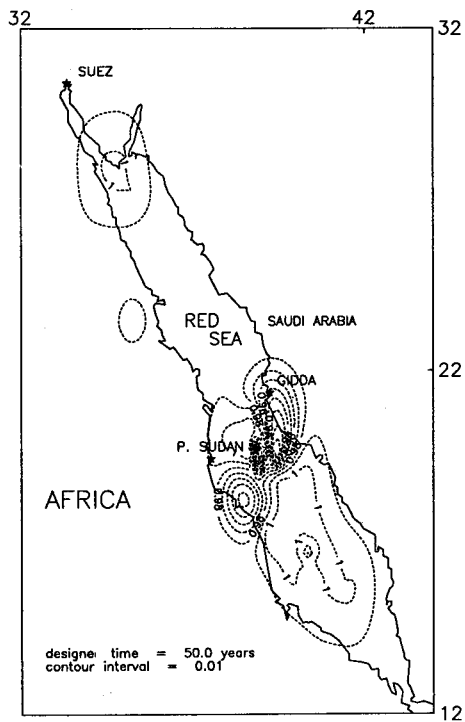


Fig. 11: Seismic risk map for design time equal to 50.0 years.

ACKNOWLEDGMENT

The author wish to thank Prof. Dr. Kijko for his assistance to execute these calculations and Prof. Dr. S. Riad for many discussions throughout the period of this work.

REFERENCES

- Abdel-Gawad, M., 1969.** Geological structures of the Red Sea area inferred from satellite pictures, In Hot brines and recent heavy deposits in the Red Sea, E. D. Degens and D. A. Ross (eds.), Springer-Verlag, N. Y., Inc., pp. 82-97.
- Barazangi, M., 1981.** Evaluation of seismic risk along the western part of the Arabian plate: discussion and recommendations, Bull. Fac. Earth. Sci., K. A. Unive., 4: 77-87.
- Burton, P. W., 1978.** Assessment of seismic hazard in the U.K., instrumentation of ground vibration and earthquakes. Institution of civil engineers, London, 35-48.
- Caputo, M., 1874.** Analysis of seismic risk. In Engineering seismology and earthquake engineering, edited by J. Solnes.
- Girdler, R. W., 1969.** The Red Sea-A geophysical background, In Hot brines and recent heavy deposits in the Red Sea, E. D. Degens and D. A. Ross (eds.), Springer-Verlag, N. Y., Inc., pp. 38-58.
- Hattori, S. and E. M. Ibrahim, 1981.** Evaluation of seismic risk in and around Egypt, Zisin, 4: 505-520.
- Heirtzler, J. R. and X. Le Pichon, 1965.** Magnetic anomalies over the Mid-Atlantic Ridge, J. Geophys. Res., 70: 4013-4018.
- Kijko, A. and M. A. Sellevoll, 1990.** Estimation of earthquake hazard parameters for incomplete and uncertain data files. Natural Hazards, 3: 1-13.
- Kijko A., 1988.** Maximum likelihood estimation of b value for uncertain magnitude values. Pure and Applied Geophysics, 126: 573-579.
- Kijko A., and M. M. Dessokey, 1987.** Application of the extreme magnitude distributions to incomplete earthquake files. Bull. Seis. Sosc. Am., 77 (4): 1429-1436.
- Lomnitz, C., 1974.** Global tectonics and earthquake risk. Elsevier Sc. Publishing. Co., N. Y.
- Mertz, H. A. and C. A. Cornell, 1973.** Seismic risk analysis based on a quadratic magnitude-frequency law. Bull. Seis. Soc. Am., 63 (6): 1999-2006.
- Riad, S. and H. Meyers, 1985.** Earthquake catalog for the middle east countries 1900-1983. World data center A for solid earth geophysics, Report SE-40.
- Prochazkova, D., B. Cuterch, A. Kijko and H. Lewandowska, 1990.** Earthquake hazard of the northern parts of the Bohemian Massif and western Carpathians, Natural Hazards, 3: 173-181.
- Said, R., 1969.** General stratigraphy of the adjacent land areas of the Red Sea. In Hot brines and recent heavy deposits in the Red Sea, E.D. Degens and D.A. Ross (eds.), Springer-Verlag, N.Y., Inc., pp. 71-81.